HHS Public Access

Author manuscript

Mov Disord. Author manuscript; available in PMC 2024 December 01.

Published in final edited form as:

Mov Disord. 2023 December ; 38(12): 2163–2172. doi:10.1002/mds.29589.

An autopsy series of seven cases of *VPS13A* disease (chorea-acanthocytosis)

Ricky M. Ditzel Jr., BSHS[1,2,3,4,5], **Ruth H. Walker, MB, ChB, PhD**[6,7,*], **Melissa J. Nirenberg, MD, PhD**[6,7], **Amber M. Tetlow, PhD**[1,2,3,4,5], **Kurt Farrell, PhD**[1,2,3,4,5], **Kourtni J. Lind-Watson**[1,2,3,4,5], **Emma L. Thorn, MA**[1,2,3,4,5], **Diana K. Dangoor, BA**[1,2,3,4,5], **Ronald Gordon, PhD**[1], **Claudia De Sanctis, PhD**[1,2,3,4,5], **Brandon Barton, MD, MS**[8,9], **Barbara I. Karp, MD**[10], **Alana Kirby, MD, PhD**[9], **Debra J. Lett, BA**[11], **Karin Mente, MD**[12,13], **David K. Simon, MD, PhD**[14,15], **Antonio Velayos-Baeza, PhD**[16,17], **Gabriel Miltenberger-Miltenyi, MD, PhD**[18,19,20,21], **Jack Humphrey, PhD**[3,4,6,22], **John F. Crary, MD PhD**[1,2,3,4,5,*]

[1]Department of Pathology, Molecular, and Cell Based Medicine, Icahn School of Medicine at Mount Sinai, New York, New York, USA.

[2]Department of Artificial Intelligence & Human Health, Icahn School of Medicine at Mount Sinai, New York, New York, USA.

[3]Nash Family Department of Neuroscience, Icahn School of Medicine at Mount Sinai, New York, NY, USA.

[4]Friedman Brain Institute, Ronald M. Loeb Center for Alzheimer's Disease, Icahn School of Medicine at Mount Sinai, New York, New York, USA.

[5]Neuropathology Brain Bank & Research CoRE, Icahn School of Medicine at Mount Sinai, New York, New York, USA.

[6]Department of Neurology, Icahn School of Medicine at Mount Sinai, New York, New York, USA.

[7]James J. Peters Veterans Affairs Medical Center, Bronx, NY, USA

[8]Rush University Medical Center, Chicago, Illinois, USA

[9]Jesse Brown Veterans Affairs Medical Center, Chicago, Illinois, USA

[10]Human Motor Control Section, National Institute of Neurological Disorders and Stroke, National Institutes of Health, Bethesda, Maryland, USA

[11]Newcastle Brain Tissue Resource, Newcastle University, Newcastle, UK

[*]Address for correspondence: Ruth H. Walker, MB, ChB, PhD, James J. Peters Veterans Affairs Medical Center, 130 W Kingsbridge Rd, Bronx, NY 10468, USA / Tel: +01-718-584-9000-x5915 / Fax: +01-718-741-4708 /, ruth.walker@mssm.edu, John F. Crary, MD-PhD, Professor, Departments of Pathology, Artificial Intelligence & Human Health & Neuroscience, Friedman Brain Institute, Ronald M. Loeb Center for Alzheimer's Disease, Icahn School of Medicine at Mount Sinai, 1 Gustave L. Levy Place Box 1194, New York, NY 10029, Office: (212) 659-8695, john.crary@mountsinai.org.

AUTHORS' ROLES

RMD, RHW, MJN, AMT, and JFC designed the study, executed the methods referenced in the manuscript, analyzed all data, and wrote and edited the manuscript. KF, JH, KLW, GMM, and AVB assisted in the interpretation of the genetic analysis and edited the final version of the manuscript. ELT was responsible for banking all brain tissues at the Mount Sinai Neuropathology Brain Bank & Research CoRE and edited the final version of the manuscript. BB, BIK, AK, DJL, KM, and DKS donated human post-mortem brain tissue to be analyzed, provided clinical information, and edited the final version of the manuscript. DKD and CD performed the immunohistochemical methods described in the manuscript and edited the final versions. RG performed TEM and edited the manuscript.

[12]Departments of Neurology and Pathology, Case Western Reserve University, Cleveland, OH, USA

[13]Louis Stokes Cleveland VA Medical Center, Cleveland OH, USA

[14]Beth Israel Deaconess Medical Center, Boston, Massachusetts, USA

[15]Harvard Medical School, Boston, Massachusetts, USA

[16]Department of Physiology, Anatomy, and Genetics, University of Oxford, UK

[17]Wellcome Centre for Human Genetics, University of Oxford, Oxford, UK

[18]Laboratório de Genética, Faculdade de Medicina, Universidade de Lisboa, Lisbon, Portugal

[19]Department of Neurology, Ludwig-Maximilians-Universität München, Munich, Germany

[20]Reference Center on Lysosomal Storage Diseases, Hospital Senhora da Oliveira, Guimarães, Portugal

[21]Instituto de Medicina Molecular João Lobo Antunes, Faculdade de Medicina da Universidade de Lisboa, Lisbon, Portugal

[22]Department of Genetics and Genomic Sciences & Icahn Institute for Data Science and Genomic Technology, Icahn School of Medicine at Mount Sinai, New York, NY, USA

Abstract

Background: Vacuolar protein sorting 13 homolog A (*VPS13A*) disease, historically known as chorea-acanthocytosis, is a rare neurodegenerative disorder caused by biallelic mutations in *VPS13A,* usually resulting in reduced or absent levels of its protein product, VPS13A. VPS13A localizes to contact sites between subcellular organelles, consistent with its recently identified role in lipid transfer between membranes. Mutations are associated with neuronal loss in the striatum, most prominently in the caudate nucleus, and associated marked astrogliosis. There are no other known disease-specific cellular changes (e.g., protein aggregation). But autopsy reports to date have been limited, often lacking genetic or biochemical diagnostic confirmation.

Methods: In this study, we collected brain tissues and clinical data from seven cases of *VPS13A* for neuropathological analysis. The clinical diagnosis was confirmed by the presence of *VPS13A* mutations and/or immunoblot showing the loss or reduction of VPS13A protein. Tissues underwent routine, special, and immunohistochemical staining focused on neurodegeneration. Electron microscopy was performed in one case.

Results: Gross examination showed severe striatal atrophy. Microscopically, there was neuronal loss and astrogliosis in affected regions. Luxol fast blue staining showed variable lipid accumulation with diverse morphology, that was further characterized by electron microscopy. In some cases, rare degenerating p62- and ubiquitin-positive cells were present in affected regions. Calcifications were present in four cases, being extensive in one.

Conclusions: We present the largest autopsy series of biochemically- and genetically-confirmed *VPS13A* disease and identify novel histopathological findings implicating abnormal lipid accumulation.

Keywords

VPS13A; chorea-acanthocytosis; neuroacanthocytosis; neuropathology; lipid

INTRODUCTION

VPS13A disease (chorea-acanthocytosis) is a rare autosomal recessive neurodegenerative disorder with typical onset of neurological symptoms usually in young adulthood [1]. Patients present with a spectrum of neurological, psychiatric, and cognitive symptoms related to basal ganglia degeneration, similar to those in Huntington's disease (HD). Hyperkinetic movement disorders are a prominent feature of *VPS13A* disease, including dystonia (particularly feeding dystonia), chorea, and tics. Additional features may include dysarthria, dysphagia, seizures, and peripheral neuromyopathy.

VPS13A disease is caused by biallelic mutations in the vacuolar protein sorting 13 homolog A (*VPS13A*) [2,3]. Mutations in other *VPS13* homologs (B-D), have been linked to other neurodegenerative diseases such as Cohen syndrome, early-onset Parkinson's disease, and spastic ataxia[4–7]. Recent studies based upon visualization of protein structure indicate that VPS13A belongs to the newly-defined superfamily of "bridge-like lipid transfer proteins" (BLTPs)[8,9], suggesting that disordered bulk transfer of lipids may play a role in disease pathophysiology.

VPS13A mutations include missense variants, deletions, and duplications, usually resulting in absent or markedly depleted levels of the protein product, VPS13A (also termed "chorein"). There is no evidence to date of genotype-phenotype correlation in *VPS13A* disease[10]. Recent evidence from animal and cellular models suggests that VPS13A is involved in trafficking of lipids between subcellular organelles including mitochondria, lipid droplets, and endoplasmic reticulum[11–17]. Cell culture studies indicate that loss of VPS13A results in decreased levels of lipid droplets, which are involved in storage of lipids as a critical step in subcellular metabolism[18]. Our group has recently demonstrated significant alterations in lipid levels in human post-mortem tissue from patients with *VPS13A* disease[19]. Further work examining alterations in lipid processing following *VPS13A* mutation in the human brain has the potential to reveal mechanisms driving striatal degeneration.

Neuropathological reports to date have described findings in single cases or small series[2,3,20–28]. Interpretation of older publications is compromised by the absence of definitive genetic- or protein-based diagnostic confirmation[29]. The consistent neuropathological findings are limited to marked neuronal loss in the basal ganglia, most prominently in the caudate nucleus (CN), with a prominent astrocytic response. There has been no evidence of protein aggregations or any other specific neuropathological cellular hallmark. Here we describe the neuropathological findings in the largest series to date of patients with *VPS13A* disease, including revisiting two previously published cases[20,22]. We identify and describe novel pathological features suggesting a possible role for VPS13A in lipid metabolism and autophagy.

METHODS

Tissue samples

Formalin-fixed, paraffin-embedded tissues were obtained from the following centers: Columbia University, New York City, New York, USA; Newcastle Brain Tissue Resource at Newcastle University, UK; Rush University, Chicago, Illinois, USA; National Institutes of Health (NIH), Bethesda, Maryland, USA; and the Neuropathology Brain Bank at the Icahn School of Medicine at Mount Sinai. Appropriate consents were obtained from the patients and next-of-kin. Regions investigated included the head of the CN, the putamen at the level of the anterior commissure, globus pallidus (GP), dorsolateral prefrontal cortex (DLPFC), superior temporal gyrus, substantia nigra (SN), hippocampus, inferior parietal cortex, and primary visual cortex.

Neuropathological assessments

Retrospective gross neuropathological assessments were not possible in most cases (Supplemental table 1). Sections were cut at 5 μm thickness and mounted on positively-charged microscope slides. Immunohistochemistry was conducted by using the Ventana Benchmark XT automatic stainer (Rouche, Tucson, AZ) for markers of abnormal phospho-tau (AT8, 1:1000, Invitrogen), amyloid β (4G8, 1:8000, Biolegend), α-synuclein (LB509, 1:3000, Abcam), TAR DNA-binding protein 43 (TDP-43, polyclonal, 1:5000, Proteintech) p62/SQSTM1 (3/p62 LCK Ligand, 1:50, BD Transduction Laboratories), ubiquitin (UB-1, 1:1000, Invitrogen), microglia (CD68, 1:1000, Millipore), and astrocytes (GFAP, 1:10, Ventana). Additional stains included silver staining (Bielschowsky), hematoxylin and eosin (H&E), and H&E counterstained with Luxol fast blue (LFB). Neuropathological scoring included tau Braak Staging, a Consortium to Establish a Registry for Alzheimer's disease (CERAD) score, Thal phase, McKeith's staging of dementia with Lewy bodies, and limbic-predominant age-related TDP-43 encephalopathy[30–36]. Slides were scored semi-quantitatively (+/− = rare, 1+ = mild, 2+ = moderate, 3+ = severe).

Electron microscopy

Human brain tissue was fixed in 4% glutaraldehyde. The sections were cut and placed in 3% glutaraldehyde with 0.2 M sodium cacodylate buffered at pH 7.4, treated with 1% osmium tetroxide for 2 hours, dehydrated in ethanol steps to 100%, and processed for embedding in Epon, Embed 812. They were treated with propylene oxide and transitioned to Epon and polymerized in a 70^{o}C oven overnight. The tissue blocks were sectioned at 1 micron, stained with methylene blue and Azure II and observed by light microscopy. Smaller representative areas were chosen for ultrathin sectioning and stained with Uranyless Lanthanum and lead citrate stain. The sections were photographed with a Hitachi H7800 transmission electron microscope (TEM) equipped with a SIA digital imaging system.

Genetic analysis

Genetic analyses for two of the cases are reported here for the first time. For case 3, DNA was isolated on the Kingfisher system (ThermoFisher) and sequenced using Illumina HiSeq as previously described[37]. FASTQ files were analyzed using the Integrated Genome

Browser (IGV) human genome 38 (GRCH38)[38]. For case 6, *VPS13A* DNA, RNA, and protein were analyzed as previously described, using relevant oligonucleotides[39]. *VPS13A* mutations in cases 1[20,40], 4[41], and 5[2] were documented as previously reported, adjusting the nomenclature to current standards. Cases 2 and 7 were only diagnosed by VPS13A Western blot analysis[42]

RESULTS

Seven subjects (three female) were included in the study (Table 1). The age of disease onset was in the 20s-30s for all subjects. Detailed clinical data were available for six of these seven cases (cases 1–3 and 5–7). Neuroimaging results were not available for all cases, but in most cases were available only in summary. The mean age of onset was 31.5 years (range 25–39 years), and the mean disease duration was 19.5 years (range 6–28 years). These six subjects had the following clinical features: chorea; orolingual dystonia (with or without other types of dystonia); tics or stereotypies; dysarthria or aphonia; dysphagia; cognitive deficits; psychiatric disturbances; and hyporeflexia/areflexia. The cause of death was aspiration pneumonia for case 1, cardiac arrest/arrhythmia for cases 2 and 6, and not reported for the others. The clinical diagnosis was confirmed by the presence of *VPS13A* mutations in five cases (1, 3–6), and reduced or absent chorein levels in two (2 and 7)[42].

Gross examination, when possible, demonstrated marked atrophy of the CN and putamen (Figure 1). Other gross signs of neurodegeneration were generally absent, but variable. For example, the hippocampus was severely atrophic in one individual (case 1) and mildly atrophic in two others (2 and 5). Microscopically, there was significant neuronal loss and astrogliosis in the CN and variably in the putamen noted on Luxol fast blue counterstained hematoxylin & eosin (LH&E) stained sections that could be highlighted by immunohistochemistry for glial fibrillary acidic protein (GFAP; Figure 1, Table 2). The GP was relatively preserved. The SN exhibited variable but minimal neuronal loss, with rare melanophages and astrogliosis. Rare vacuolated neurons were also observed. There were notable mineralized neurons found in the CN, putamen, and SN of cases 2, 4, 5, and 7. This mineralization had various morphologies, including a distinctive pattern of perineuronal prominence in some cases. This was seen alongside more typical perivascular calcospherites and other common morphologies.

Other microscopic changes included accumulation of autophagy-associated proteins p62 and ubiquitin variably in all cases (Figure 2, Table 2). One case (case 1) had severe p62 and ubiquitin accumulation in the hippocampus with mild accumulation in the CN and putamen. Age-related changes were also seen in the older subjects (ages 51–61). Sparse neurofibrillary tangles (NFTs) were found in the hippocampal formations of cases 3 and 5. Case 5 also had moderate NFTs in the midbrain and upper pons (with associated glial tau inclusions). The other cases were negative for tau pathology. Diffuse amyloid plaques were found in the frontal cortex and hippocampal formations of case 2 and case 5. Case 2 had mild neuritic plaques in the frontal cortex. One individual (case 1) had mild Lewy body pathology, while another (case 5) had an abnormal ballooning cell with α-synuclein positivity in the SN and abnormal perivascular positivity in the pons, but typical Lewy

body-type inclusions were not evident (Figure 2). All cases were negative for TDP-43 inclusions.

In five of six cases, robust LFB-positive intraneuronal accumulations with diverse morphologies were noted in multiple brain regions (Figure 3, Table 2), especially the CN and putamen, but also in other regions, including the parietal cortex and amygdala, which was noted to be hyperintense on T2 MRI in case 1. Many cells exhibited irregular and large LFB-positive puncta; these could be seen intermixed with LFB-negative lipofuscin pigment in some cells. In contrast, other cells displayed more finely granular staining patterns either localized or diffusely in the cytoplasm. Three cases had LFB-positive accumulations in the hippocampus, and in two they were observed in the GP. On transmission electron microscopy (TEM) these were observed to be frequent electron-dense globular intracytoplasmic structures (Figure 3).

DISCUSSION

Here we report novel neuropathological findings in the largest autopsy case series of *VPS13A* disease to date. Little is known about the neuropathology of *VPS13A* disease on the cellular level beyond the vulnerability of the striatum, which displayed severe neurodegenerative changes with marked neuronal loss and astrogliosis in all cases we studied. The particular vulnerability of the CN in *VPS13A* disease[25,43] is not well understood and is a critical knowledge gap as it has the potential to shed light on neurodegeneration in other choreas, including HD. However, in contrast to HD, the head of the caudate nucleus appears to be especially vulnerable, which may relate to some of the specific behavioral issues[25,43] In addition to CN and putaminal atrophy, we report heterogenous neuropathological findings that include age-related degenerative changes (e.g., inclusions) and other observations. Variable yet robust LFB-positive intra-cytoplasmic accumulations were observed and might be related to abnormalities in lipid processing that have been linked to *VPS13A* mutations in animal and cellular models [44,45].

VPS13A protein has been reported to localize to contact sites between the endoplasmic reticulum (ER) and mitochondria and to facilitate lipid transport resembling the ER-mitochondria encounter systems (ERMES) seen in yeast[17], in addition to playing an important role in formation of lipid droplets, critical for regulation of lipid metabolism[18]. Impairment of phosphorylation was noted in erythrocytes from patients with VPS13A disease[46]. Recently, *in silico* prediction models have provided further details of the structure and apparent function of VPS13A in lipid transport between subcellular organelles[13,47], as part of the group of related proteins (BLTPs) fulfilling similar functions[8,9]. An ongoing lipidomics study by our group (including cases 1–4 in this study) demonstrated elevated levels of bis(mono-acylglycerol) phosphate (BMP), sulfatide, lysphosphatidylserine, and phosphatidylcholine in the CN and putamen, but not in the DLPFC, of human brain tissue[19]. Our electron microscopy results are compatible with intraneuronal lipid accumulation with the caveat, however, that we could not conclusively confirm the constituents of these inclusions.

Recent evidence demonstrates that loss of function of VPS13A impairs autophagic mechanisms in disease models[44,45] and in circulating erythrocytes from affected patients[46]. P62- and ubiquitin-immunoreactive inclusions were variable, but most abundant in the hippocampus in our cases while the striatum contained only occasional inclusions. It is possible that the lipid accumulation in the form of lipid droplets could enhance the autophagy pathway by promoting the initiation of the autophagosome. Disruption of this pathway is known to have detrimental effects, including neuronal death[17,48–50]. Autophagy-related proteins may not be easily appreciated in regions where there is severe neuronal loss, as seen in the CN and putamen in *VPS13A* disease.

Consistent with previous reports, we did not find any evidence that *VPS13A* disease is characterized by the types of abnormal protein accumulations seen in other neurodegenerative diseases[20,22,23]. The finding in one case of brainstem-predominant Lewy body pathology appeared to be clinically incidental, as can be seen in approximately 24% of healthy elderly individuals[51]. Similarly, the presence of Alzheimer's disease neuropathological changes were consistent with early degenerative changes that are common in this age range[31] and thus were likely also an incidental finding. The significance of the mineralization is unclear. The mineralization differs from mineralizing lenticulostriate vasculopathy, and pericapillary calcospherites because of its location around neurons. It also differs from neuronal mineralization occurring in the perinatal period in which neurons are replaced by mineralized "fossils"[52]. The pattern of deposition seen in our cases bears some resemblance to regional encephalic mineralization seen in mitochondriopathy in Jack Russell Terrier dogs[53]. Further studies are required to elucidate the significant of this unusual finding.

Strengths of our study include the size of the cohort, our detailed clinical and genetic documentation, and the extensive histopathological characterization including findings of mineralization, LFB-positive accumulations, and autophagy-associated proteins. Limitations include potential selection bias, variability in brain banking protocols, post-mortem interval, and fixation times (Supplemental table). While all subjects had features typical of *VPS13A* disease, there was heterogeneity in the underlying genetic mutations, clinical presentation, and disease course and duration. The constituents of the observed LFB-positive accumulations could not be definitively confirmed using the current techniques. Tissue appropriate for TEM was available for only one case. Further studies are therefore warranted to confirm and extend these findings.

This autopsy series, the largest of its kind, provides novel insights into the possible mechanisms underlying *VPS13A* disease and other diseases caused by mutations in the *VPS13* gene family. Future neuropathological studies in larger cohorts, combined with other methodologies such as transcriptomics and proteomics, are needed to further characterize these findings. Advancing our understanding of the neuropathology of *VPS13A* disease remains an urgent priority given its promise to shed light on the cell death-related mechanism underlying the selective vulnerability in the choreas and may lead to strategies to develop therapeutic interventions.

Supplementary Material

Refer to Web version on PubMed Central for supplementary material.

Acknowledgments:

We are most grateful to the patients and families affected by *VPS13A* disease (chorea-acanthocytosis) who made this work possible. The study was supported by a grant from Neuroacanthocytosis Advocacy USA. We thank the staff of the contributing centers and institutes. Additionally, we would like to acknowledge the Neuropathology Brain Bank & Research CoRE at the Icahn School of Medicine at Mount Sinai and especially Valeriy Burokhov. We acknowledge the following additional funding sources: NIH grants R01AG054008, R01NS095252, RF1AG060961, R01NS086736, R01AG062348, RF1MH128969, P30AG066514, R01AG063819, R01NS116006, U54NS115266, and the Rainwater Charitable Foundation. Western blot analysis for VPS13A (chorein) was supported by funding from the Advocacy for Neuroacanthocytosis Patients (www.naadvocacy.org) and the EMINA network (www.erare.edu/financed-projects/emina) and was performed in the labs of Profs. Kretzschmar, Giese, Herms (Neuropathology) and Danek (Neurology) at Ludwig-Maximilians-Universität Munich, Germany.

FINANCIAL DISLOSURES

RMD participated under contract for the Congressionally Directed Medical Research Program (CDMRP) in 2023 and consulted for Vigilant Consulting. RHW receives research funding from the Department of Veterans Affairs (CSRD Merit Award CX002342), consulted for Teladoc, Inc. and received an honorarium from New York University (NYU) Medical Center. MJN receives research funding from the Department of Veterans Affairs (CSRD Merit Award CX002342), received an honorarium from the Parkinson's Foundation, International Parkinson and Movement Disorder Society. AVB is supported by a grant from the Wellcome Trust (0930532/Z/09/Z). KF participated under contract for the CDMRP. AMT is supported by a T32 Postdoctoral Research Training Program in Alzheimer's Disease and Related Neurodegenerative Disorders ((T32AG052909 Wisniewski, Scharfman). AK received funding from NINDS R21 (NS127037), the Cohn Family Foundation (Cohn Fellowship), Postma Family (Pilot Award), and salary support from Rush University Medical Center. KM was supported by a clinical research fellowship from the Dystonia Medical Research Foundation and is currently supported by the Cleveland Alzheimer's Disease Research Center (P30-AG072959). DS is on the advisory board for Weston Brain Institute; Cure Parkinson's Trust. He worked under contract for Neuraly (for participate as a site for a clinical trial), received an honorarium from the NIH for "PD-BRAC", and has a grant from the Weston Institute, NIH, Parkinson's Foundation, and research support from the Owens Family Foundation. BK, DL, and KLW have no financial disclosures. JFC is supported by Neuroacanthocytosis Advocacy, the Rainwater Charitable Foundation, and the NIH (grants R01AG054008, R01NS095252, RF1AG060961, R01NS086736, R01AG062348, RF1MH128969, P30AG066514, R01AG063819, R01NS116006, U54NS115266).

REFERENCES

1. Peikert K et al. VPS13A Disease. in GeneReviews® (eds. Adam MP et al.) (University of Washington, Seattle, 1993).
2. Rampoldi L et al. A conserved sorting-associated protein is mutant in chorea-acanthocytosis. Nat. Genet. 28, 119–120 (2001). [PubMed: 11381253]
3. Ueno S et al. The gene encoding a newly discovered protein, chorein, is mutated in chorea-acanthocytosis. Nat. Genet. 28, 121–122 (2001). [PubMed: 11381254]
4. Kolehmainen J et al. Cohen syndrome is caused by mutations in a novel gene, COH1, encoding a transmembrane protein with a presumed role in vesicle-mediated sorting and intracellular protein transport. Am. J. Hum. Genet. 72, 1359–1369 (2003). [PubMed: 12730828]
5. Lesage S et al. Loss of VPS13C Function in Autosomal-Recessive Parkinsonism Causes Mitochondrial Dysfunction and Increases PINK1/Parkin-Dependent Mitophagy. Am. J. Hum. Genet. 98, 500–513 (2016). [PubMed: 26942284]
6. Seong E et al. Mutations in VPS13D lead to a new recessive ataxia with spasticity and mitochondrial defects. Ann. Neurol. 83, 1075–1088 (2018). [PubMed: 29604224]
7. Gauthier J et al. Recessive mutations in VPS13D cause childhood onset movement disorders. Ann. Neurol. 83, 1089–1095 (2018). [PubMed: 29518281]
8. Neuman SD, Levine TP & Bashirullah A A novel superfamily of bridge-like lipid transfer proteins. Trends Cell Biol. 32, 962–974 (2022). [PubMed: 35491307]

9. Braschi B, Bruford EA, Cavanagh AT, Neuman SD & Bashirullah A The bridge-like lipid transfer protein (BLTP) gene group: introducing new nomenclature based on structural homology indicating shared function. Hum. Genomics 16, 66 (2022). [PubMed: 36461115]
10. Lossos A et al. Early clinical heterogeneity in choreoacanthocytosis. Arch. Neurol. 62, 611–614 (2005). [PubMed: 15824261]
11. Dziurdzik SK & Conibear E The Vps13 Family of Lipid Transporters and Its Role at Membrane Contact Sites. Int. J. Mol. Sci. 22, 2905 (2021). [PubMed: 33809364]
12. Yeshaw WM et al. Human VPS13A is associated with multiple organelles and influences mitochondrial morphology and lipid droplet motility. eLife 8, e43561 (2019). [PubMed: 30741634]
13. Park J-S, Hu Y, Hollingsworth NM, Miltenberger-Miltenyi G & Neiman AM Interaction between VPS13A and the XK scramblase is important for VPS13A function in humans. J. Cell Sci. 135, jcs260227 (2022). [PubMed: 35950506]
14. Adlakha J, Hong Z, Li P & Reinisch KM Structural and biochemical insights into lipid transport by VPS13 proteins. J. Cell Biol. 221, e202202030 (2022). [PubMed: 35357422]
15. Ryoden Y, Segawa K & Nagata S Requirement of Xk and Vps13a for the P2X7-mediated phospholipid scrambling and cell lysis in mouse T cells. Proc. Natl. Acad. Sci. U. S. A. 119, e2119286119 (2022). [PubMed: 35140185]
16. Guillén-Samander A et al. A partnership between the lipid scramblase XK and the lipid transfer protein VPS13A at the plasma membrane. Proc. Natl. Acad. Sci. U. S. A. 119, e2205425119 (2022). [PubMed: 35994651]
17. Kumar N et al. VPS13A and VPS13C are lipid transport proteins differentially localized at ER contact sites. J. Cell Biol. 217, 3625–3639 (2018). [PubMed: 30093493]
18. Chen S et al. VPS13A and VPS13C Influence Lipid Droplet Abundance. Contact Thousand Oaks Ventura Cty. Calif 5, 25152564221125613 (2022).
19. Miltenberger-Miltenyi G et al. Sphingolipid and phopsholipid level changes in human brain indicate defects in lipid processing in VPS13A-disease (chorea-acanthocytosis). Mov. Disord. Off. J. Mov. Disord. Soc. Online ahead of print (2023)
20. Mente K et al. Hippocampal sclerosis and mesial temporal lobe epilepsy in chorea-acanthocytosis: a case with clinical, pathologic and genetic evaluation. Neuropathol. Appl. Neurobiol. 43, 542–546 (2017). [PubMed: 28398599]
21. Connolly BS, Hazrati L-N & Lang AE Neuropathological findings in chorea-acanthocytosis: new insights into mechanisms underlying parkinsonism and seizures. Acta Neuropathol. (Berl.) 127, 613–615 (2014). [PubMed: 24394886]
22. Rinne JO et al. The neuropathological features of neuroacanthocytosis. Mov. Disord. 9, 297–304 (1994). [PubMed: 8041370]
23. Rinne JO, Daniel SE, Scaravilli F, Harding AE & Marsden CD Nigral degeneration in neuroacanthocytosis. Neurology 44, 1629–1632 (1994). [PubMed: 7936287]
24. Liu J et al. Pathoarchitectonics of the cerebral cortex in chorea-acanthocytosis and Huntington's disease. Neuropathol. Appl. Neurobiol. 45, 230–243 (2019). [PubMed: 29722054]
25. Liu J et al. Subcortical neurodegeneration in chorea: Similarities and differences between chorea-acanthocytosis and Huntington's disease. Parkinsonism Relat. Disord. 49, 54–59 (2018). [PubMed: 29402698]
26. Ishida C, Makifuchi T, Saiki S, Hirose G & Yamada M A neuropathological study of autosomal-dominant chorea-acanthocytosis with a mutation of VPS13A. Acta Neuropathol. (Berl.) 117, 85–94 (2009). [PubMed: 18584183]
27. Alonso ME, Teixeira F, Jimenez G & Escobar A Chorea-acanthocytosis: report of a family and neuropathological study of two cases. Can. J. Neurol. Sci. J. Can. Sci. Neurol 16, 426–431 (1989).
28. Bader B et al. Neuropathology of Chorea-Acanthocytosis. in Neuroacanthocytosis Syndromes II (eds. Walker RH, Saiki S & Danek A) 187–195 (Springer, 2008). doi:10.1007/978-3-540-71693-8_15.
29. Hardie RJ et al. Neuroacanthocytosis. A clinical, haematological and pathological study of 19 cases. Brain J. Neurol. 114 (Pt 1A), 13–49 (1991).

30. Thal DR, Rüb U, Orantes M & Braak H Phases of A beta-deposition in the human brain and its relevance for the development of AD. Neurology 58, 1791–1800 (2002). [PubMed: 12084879]
31. Braak H, Thal DR, Ghebremedhin E & Del Tredici K Stages of the pathologic process in Alzheimer disease: age categories from 1 to 100 years. J. Neuropathol. Exp. Neurol. 70, 960–969 (2011). [PubMed: 22002422]
32. Braak H & Braak E Neuropathological stageing of Alzheimer-related changes. Acta Neuropathol. (Berl.) 82, 239–259 (1991). [PubMed: 1759558]
33. Montine TJ et al. National Institute on Aging-Alzheimer's Association guidelines for the neuropathologic assessment of Alzheimer's disease: a practical approach. Acta Neuropathol. (Berl.) 123, 1–11 (2012). [PubMed: 22101365]
34. Braak H et al. Staging of brain pathology related to sporadic Parkinson's disease. Neurobiol. Aging 24, 197–211 (2003). [PubMed: 12498954]
35. Attems J et al. Neuropathological consensus criteria for the evaluation of Lewy pathology in post-mortem brains: a multi-centre study. Acta Neuropathol. (Berl.) 141, 159–172 (2021). [PubMed: 33399945]
36. McKeith IG et al. Diagnosis and management of dementia with Lewy bodies: Fourth consensus report of the DLB Consortium. Neurology 89, 88–100 (2017). [PubMed: 28592453]
37. Farrell K et al. Genome-wide association study and functional validation implicates JADE1 in tauopathy. Acta Neuropathol. (Berl.) 143, 33–53 (2022). [PubMed: 34719765]
38. Robinson JT et al. Integrative Genomics Viewer. Nat. Biotechnol. 29, 24–26 (2011). [PubMed: 21221095]
39. Spieler D et al. Identification of two compound heterozygous VPS13A large deletions in chorea-acanthocytosis only by protein and quantitative DNA analysis. Mol. Genet. Genomic Med. 8, e1179 (2020). [PubMed: 32056394]
40. Dobson-Stone C et al. Mutational spectrum of the CHAC gene in patients with chorea-acanthocytosis. Eur. J. Hum. Genet. EJHG 10, 773–781 (2002). [PubMed: 12404112]
41. Keogh MJ et al. Genetic compendium of 1511 human brains available through the UK Medical Research Council Brain Banks Network Resource. Genome Res. 27, 165–173 (2017). [PubMed: 28003435]
42. Dobson-Stone C et al. Chorein detection for the diagnosis of chorea-acanthocytosis. Ann. Neurol. 56, 299–302 (2004). [PubMed: 15293285]
43. Walterfang M et al. The neuropsychiatry of neuroacanthocytosis syndromes. Neurosci. Biobehav. Rev. 35, 1275–1283 (2011). [PubMed: 21237198]
44. Peikert K et al. Therapeutic targeting of Lyn kinase to treat chorea-acanthocytosis. Acta Neuropathol. Commun. 9, 81 (2021). [PubMed: 33941276]
45. Vonk JJ et al. Drosophila Vps13 Is Required for Protein Homeostasis in the Brain. PloS One 12, e0170106 (2017). [PubMed: 28107480]
46. Lupo F et al. A new molecular link between defective autophagy and erythroid abnormalities in chorea-acanthocytosis. Blood 128, 2976–2987 (2016). [PubMed: 27742708]
47. Dall'Armellina F, Stagi M & Swan LE In silico modeling human VPS13 proteins associated with donor and target membranes suggests lipid transfer mechanisms. Proteins Struct. Funct. Bioinforma. 91, 439–455 (2023).
48. Ralhan I, Chang C-L, Lippincott-Schwartz J & Ioannou MS Lipid droplets in the nervous system. J. Cell Biol. 220, e202102136 (2021). [PubMed: 34152362]
49. Velázquez AP & Graef M Autophagy regulation depends on ER homeostasis controlled by lipid droplets. Autophagy 12, 1409–1410 (2016). [PubMed: 27245853]
50. Velázquez AP, Tatsuta T, Ghillebert R, Drescher I & Graef M Lipid droplet-mediated ER homeostasis regulates autophagy and cell survival during starvation. J. Cell Biol. 212, 621–631 (2016). [PubMed: 26953354]
51. Markesbery WR, Jicha GA, Liu H & Schmitt FA Lewy body pathology in normal elderly subjects. J. Neuropathol. Exp. Neurol. 68, 816–822 (2009). [PubMed: 19535990]
52. Sobel RA Greenfield's Neuropathology, Ninth Edition: 2-Volume Set. J. Neuropathol. Exp. Neurol. 74, 1185 (2015).

53. Gruber AD, Wessmann A, Vandevelde M, Summers BA & Tipold A Mitochondriopathy with regional encephalic mineralization in a Jack Russell Terrier. Vet. Pathol. 39, 732–736 (2002). [PubMed: 12450205]

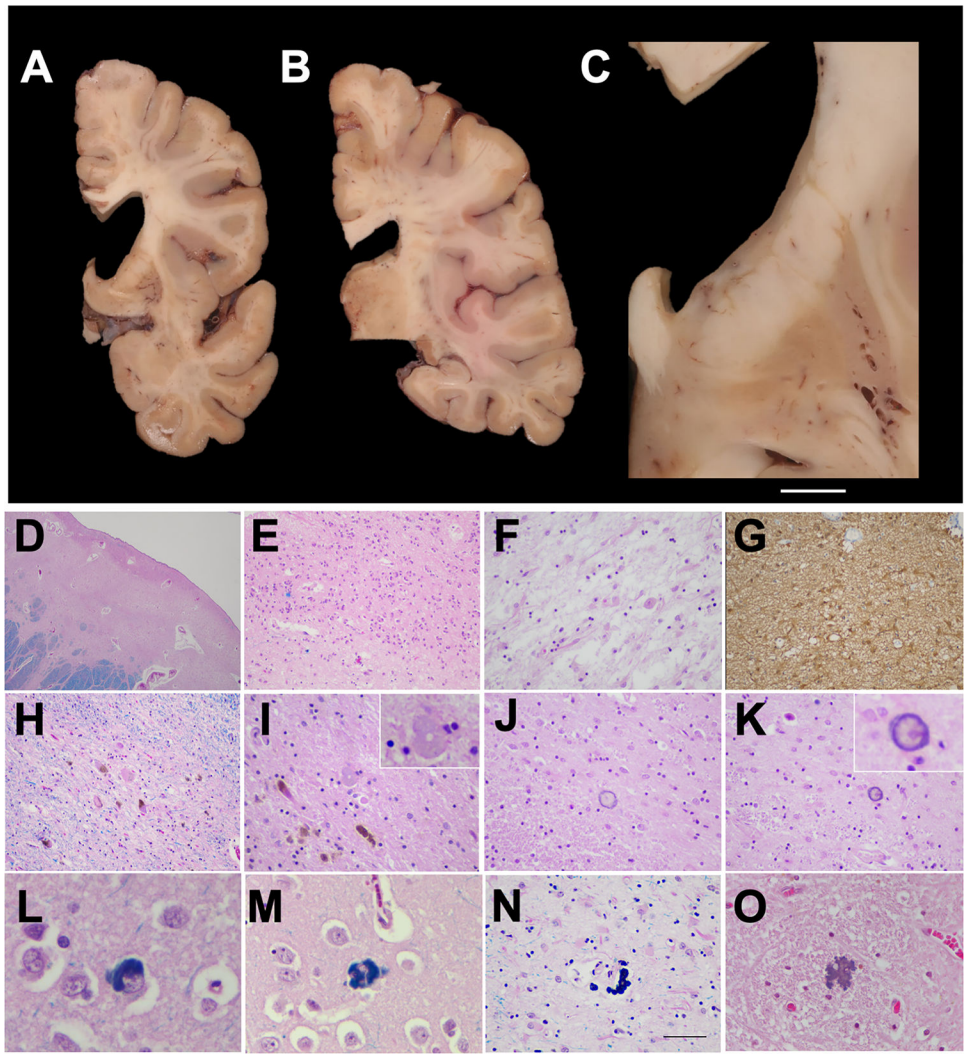

FIG. 1.

Gross neuropathology and microscopic degenerative findings of *VPS13A* disease (chorea-acanthocytosis). (**A**) Coronal hemi-brain section (right) at the level of the amygdala (case 3) showing marked atrophy of the caudate nucleus and putamen with ventricular dilatation. (**B**) Section at the level of the lateral geniculate shows an unremarkable hippocampal formation with no dilatation of the temporal horn of the lateral ventricle. (**C**) Higher power image of the striatum highlighting atrophy of the caudate with discoloration and atrophy of the putamen with prominent perivascular spaces. *Scale bar*, 2 cm (**A**, **B**), 0.5 cm (**C**). (**D**) Luxol fast blue counterstained hematoxylin & eosin (LH&E) stained sections show neuronal loss of the striatum with (**E, F**) fibrotic astroglial scarring. (**G**) Immunohistochemistry staining for glial fibrillary acidic protein (GFAP) highlights astroglial proliferation. (**H, I**) Rare vacuolated neurons were observed in the substantia nigra. (**J, K**) Neurons in the putamen (case 5) showed concentric perineuronal mineralization. (**L, M**) This case also displayed frequent cortical neurons exhibiting perineuronal mineralization. (**N)** Neuron showing a perivascular calcospherite pattern. (**O**) Non-neuronal mineralization in the white matter. 10x magnification for **D-K;** 20x magnification (**L-O**).

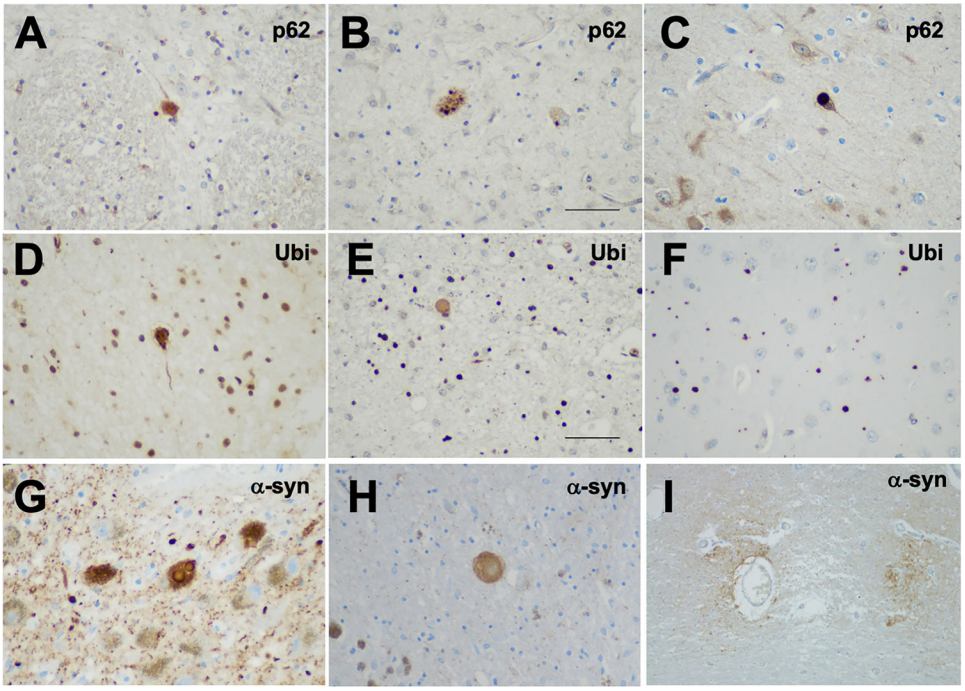

FIG. 2.

Immunohistochemistry (IHC) of autophagy and ubiquitin-proteasome protein accumulation in *VPS13A* disease (chorea-acanthocytosis). Sections show rare p62-positive cytoplasmic structures with variable morphologies, including (**A**) cytoplasmic staining in the caudate (case 2), (**B**) granular cytoplasmic staining in the putamen (case 3), and (**C**) a p62-positive (α-synuclein negative) "Lewy body-like" inclusion in the hippocampus (case 7). Ubiquitin (Ubi) immunopositive structures are seen in the neurons, neuropil, and other cells of the (**D**) caudate, (**E**) putamen, and (**F**) hippocampus. Case 1 displayed mild α-synuclein-positive Lewy bodies in the substantia nigra (**G**). Case 5 had α-synuclein positivity in a rare ballooned neuron (**H**) and rare perivascular positivity in the pons (**I**).

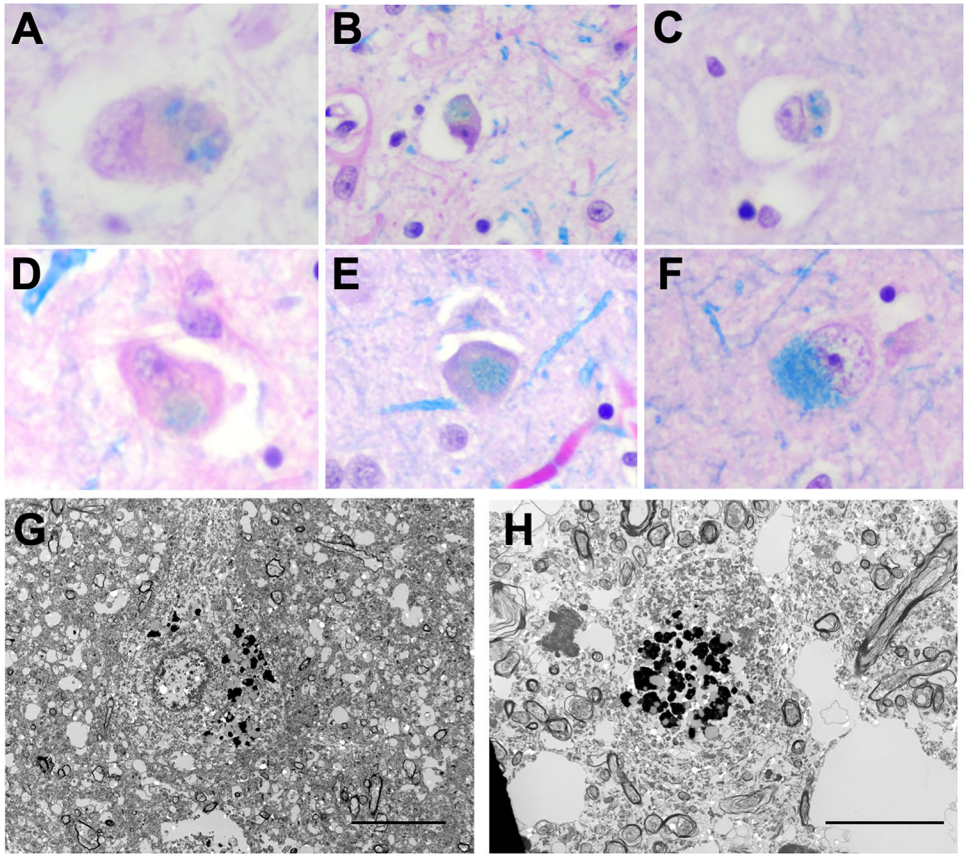

FIG. 3.

Examples of lipid accumulation morphologies in *VPS13A* disease (chorea-acanthocytosis) and transmission electron microscopy. Sections stained with Luxol fast blue (LFB) showed variable patterns of granular lipid accumulation in the striatum (**A**, **B**), and amygdala (**C**). We also observed compact cytoplasmic accumulations shown in the striatum (**D**) and parietal cortex (**E**), as well as more diffuse patterns here shown in the amygdala (**F**). 40x magnification for all images. Images illustrate robust accumulation of electron dense coarse granular material within neurons in the (**G**) dorsolateral prefrontal cortex and (**H**) putamen of case 3. Scale bar 50 mm.

TABLE 1.

Demographic, neurological and diagnostic data

Case	Age, onset / death (yr)	Sex	Movement Disorders	Bulbar	Seizure	Neuromyopathy	Cognitive	Psychiatric	Other	Labs	Brain MRI	Gene Variant
1	29 / 51	M	Chorea Dystonia: orolingual Tics	Dysarthria Dysphagia	+	Hyporeflexia ↓Vibratory sensation EMG: Diffuse axonal neurop.	Inattention Memory loss Slow processing	Anxiety Personality changes	Bradycardia/ pacemaker Esophageal dysmotility Muscle wx	Acanthocytes ↑CK (1000–4000)	BG atrophy, ↑T2 (in b/l hippocampus & amygdala)	c.3283G>C; p.(A1095P) & c.4835del; p.(P1612Qfs*30)
2	25 / 50	M	Chorea Dystonia: oromandibular Lip/tongue/ cheek biting Myoclonus (late) Parkinsonism Tics Tremor (hands)	Dysarthria/ Aphonia Dysphagia Sialorrhea	+	Areflexia	Memory loss	Depression	Muscle wx Parasomnia Sleep apnea	Acanthocytes ↑CK (2400) Western blot: ↓↓↓ Chorein	No significant findings (~10 yrs after onset)	NA
3	33 / 61	F	Cheek/lip biting Chorea Dystonia: facial (including orolingual/ oromandibular), also UE and LE Parkinsonism Tics Toe walking Tremor (hands)	Dysarthria Dysphagia Sialorrhea	+	Absent ankle jerks Normal sensation	Apraxia Bradyphrenia Memory loss	Anxiety Depression Disinhibition Emotional lability ↓Social interaction	Burning tongue Eructation Slow saccades; ↓Vertical saccade initiation	Acanthocytes ↑CK (200s-500s) Western blot: Erythrocytes ↓↓↓ Chorein	Atrophy (particularly in b/l BG and R>L medial temporal lobe)	c.2765dup p.(Y922*) & c.6404dup p.(S2136Kfs*2)
4	30s / 40	M	NA	NA	NA	NA	NA	NA	NA	NA	NA	p.(L1841*) & p.(W2347Gfs*36)
5	39 / 61	F	Chorea Dystonia: orolingual Parkinsonism Tics	Dysarthria/ Aphonia Dysphagia	–	Hyporeflexia	Dementia	Yes, unspecified	Atrophy Muscle wx Extensor plantars	↑CK (500s) Iron deficiency anemia *No acanthocytes*	Cerebral and caudate atrophy	c.269T>A; p.(I90K) & c.6404dup ; p.(S2136Kfs*2)
6	32 / 38	M	Chorea Dystonia: cervical, LE, orolingual Parkinsonism Stereotypies	Dysarthria/ Aphonia Dysphagia	– vEEG: Normal	Hyporeflexia; ↓Vibratory sensation EMG: Mild sensory neurop.	Only following simple commands (late)	Anxiety Depression Impulsivity Insomnia OCD	Eructation Headaches	Acanthocytes ↑CK (700s) ↑LFTs Western blot: ↓↓↓ Chorein	BG atrophy	c.1358-26_1358_12 delins1358-39_1358-30; p.T453Kfs*6 & c.7214T>G; p.L2405*

Case	Age, onset / death (yr)	Sex	Movement Disorders	Bulbar	Seizure	Neuromyopathy	Cognitive	Psychiatric	Other	Labs	Brain MRI	Gene Variant
7	28 / 45	F	Chorea Dystonia: axial, cervical limb, orolingual Hypomimia Stereotypies Tics Tongue/lip biting	Dysarthria Dysphagia	+ vEEG: Intermittent left slowing	Hyporeflexia ↓Vibratory sensation EMG: Absent H reflexes	Dementia ↓Attention ↓Executive fn ↓Processing ↓Working memory	Depression	Muscle wasting Migraines Spastic gait	Acanthocytes ↓Albumin ↑CK (500s) ↓Protein Western blot: ↓↓↓ Chorein	No parenchymal abnormalities	NA

Abbreviations: BG, basal ganglia; b/l, bilateral; ↓↓↓ Chorein, markedly reduced or absent chorein; CK, creatinine kinase; fn, function; INDEL/DELIN, insertion/deletion; neurop, neuropathy; UE, upper extremity; LE, lower extremity; OCD, obsessive-compulsive disorder; R, right; ↑T2, T2 hyperintensity; vEEG, video electroencephalography; NA, not available. Previously published cases include: Case 1[20,40]; Case 4 no specific changes at the DNA level were reported in the original publication[41]; Case 5[2,22,23].

TABLE 2.

Selective vulnerability in *VPS13A* disease (chorea-acanthocytosis)

Case	*Hippocampus*						*Caudate*						*Putamen*						*Glob*		
	NL	**GFAP**	**CD68**	**Lipid**	**p62**	**Ub**	**NL**	**GFAP**	**CD68**	**Lipid**	**p62**	**Ub**	**NL**	**GFAP**	**CD68**	**Lipid**	**p62**	**Ub**	**NL**	**GFAP**	**CD**
1	+++	+++	+++	−	+++	+++	+++	+++	+	+	+	+	+++	++	+	+	+	+/−	−	−	+
2	+	++	+	+	+	+	+++	+++	+	+	+/−	+/−	+++	++	+	+	+/−	+/−	−	+	
3	−	+++	−	+	+	+	+++	+++	++	+	−	−	+++	+++	++	+++	−	−	−	+++	+
4	++	NA	NA	NA	NA	NA	+++	NA	NA	NA	NA	NA	++	NA	NA	NA	NA	NA	NA	NA	N
5	+	+++	++	−	+	+++	+++	+++	++	+	−	+	+++	++	++	+	−	++	NA	NA	N
6	−	++	+	+	+	+	NA	+++	+	+	−	+/−	+++	++	+	+	−	+	−	+	
7	−	+++	++	−	+	+	+++	+++	+	−	+	+	++	+	+	−	+	+	NA	NA	N

Neuronal loss (NL) was scored on hematoxylin & eosin stain (H&E) or with Luxol fast blue counterstain (LH&E). Immunohistochemistry was not performed on case 4.

$^{\Delta}$Only in white matter.

Lipid accumulation is defined by presence of abnormal LFB. For Case 4, only H&E available for review. Immunohistochemistry markers: GFAP, glial fibrillary acidic protein; CD68, cluster differentiation 68; Ub, ubiquitin. NA, not available.